Biocatalysis and Agricultural Biotechnology 45 (2022) 102490

Contents lists available at ScienceDirect

Biocatalysis and Agricultural Biotechnology

journal homepage: www.elsevier.com/locate/bab

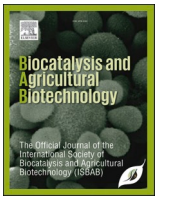

Multi-objective optimal control of Docosahexaenoic Acid (DHA) production in fed-batch fermentation by Schizochytrium sp.

F.S. Rohman [a], M.F. Roslan [b], D. Muhammad [a], N.F. Shoparwe [b,*], A.A. Hamid [c]

[a] School of Chemical Engineering, Universiti Sains Malaysia, Engineering Campus, Seri Ampangan, 14300, Nibong Tebal, Pulau Pinang, Malaysia
[b] Faculty of Bioengineering and Technology, Jeli Campus, Universiti Malaysia Kelantan, 17600, Jeli Kelantan, Malaysia
[c] Department of Biological Sciences and Biotechnology, Universiti Kebangsaan Malaysia, 43600, Bangi, Selangor, Malaysia

ARTICLE INFO

Keywords:
Docosahexaenoic acid
Bioreactor
Fermentation
Optimal control
Hybrid strategy
Control vector parameterization
Multi-objective optimi
z
ation

ABSTRACT

Docosahexaenoic Acid (DHA) production from fermentation process in a fed-batch reactor is suited solved using optimal control to obtain optimal temperature and feed flowrate trajectories. This fermentation process, which involves numerous conflicting objectives, necessitates the solution of a multi-objective optimal control (MOOC). MOOC results, which include a variety of ideal solutions, are configured as Pareto Front (PF). The ε-constraint with hybrid strategy (HS), and elitist non-dominated sorting genetic algorithm (NSGA-II) have been implemented to tackle conflict bi-objectives: minimisation final time and maximizing DHA production. By computing performance measurements such as space (SP), hypervolume (HV), and pure diversity (PD), these MOOC techniques were compared to the characteristic of the Pareto solution. Due to the most precise, diverse, and desirable spread points along the PF, the ε-constraint technique is the most effective. Each Pareto solution point comprises a unique combination of optimal feed flowrate trajectories, resulting in a unique amount of final time and DHA concentration. These solutions provide a variety of options for evaluating trade-offs and establishing the best operating strategy.

1. Introduction

Docosahexaenoic Acid (DHA) is one of a polyunsaturated fatty acid. DHA often consumed through food such as in mackerel, salmon and cod which is rich in DHA because mammals could not synthesize it efficiently due to lack of specific enzymes to produce double bond at the ω-3 position which is needed when converting α-linolenic acid (ALA) to DHA (Hishikawa et al., 2017). Polyunsaturated fatty acid is a fatty acid that contains two or more double bond between the carbon that can be seen in its chemical structure which is shown in Fig. 1 (Dominguez and Barbagallo, 2018). Polyunsaturated fatty acid consists of carbon and hydrogen that exist in fatty acyl chain with double bond that contributes to kink structure and carboxyl (COOH) group which is located at the terminal. Two main polyunsaturated fatty acids are omega-3 fatty acids and omega-6 fatty acids where DHA is an example of omega-3 fatty acid. The number in the two main polyunsaturated fatty acids indicates the space ω-carbon which is the carbon in the terminal methyl group with the first double bond. DHA has 22 carbons in its acyl chain and 6 cis double bond which is the double bond that occurs on the same side. This characteristic contributes to the low melting point properties (Calder, 2016).

During the fermentation process, the production of DHA is often limited by the carbon source, especially in batch fermentation mode. Low concentration of carbon source will reduce the cell growth whereas high concentration of carbon source can inhibit the cell

* Corresponding author.
E-mail address: fazliani.s@umk.edu.my (N.F. Shoparwe).

https://doi.org/10.1016/j.bcab.2022.102490
Received 22 April 2022; Received in revised form 3 August 2022; Accepted 12 September 2022
Available online 3 October 2022

growth. Fed-batch fermentation is an alternative strategy to increase the production of DHA as it maintains the optimum concentration of carbon source during the start of fermentation and provides excess carbon source in the middle of the fermentation process. This can improve DHA production as the lipid accumulation is associated with excess carbon source supply and nitrogen starvation in oleaginous microorganisms (Qu et al., 2013). Feeding strategy in fed-batch fermentation is one of the aspects that could help in improving the DHA yield. Fed-batch fermentation has the potential to increase the production of DHA in Schizochytrium sp. as fed-batch fermentation could provide additional nutrients that batch fermentation could not provide which results in different metabolic pathways in the production of DHA. Many feeding strategies can be applied for the production of DHA during fed-batch fermentation. Two basic models were classified which are with feedback control and without feedback control. Operation without feedback control in fed-batch fermentation includes intermittent fed-batch, constant rate fed-batch, exponentially fed-batch and optimized fed-batch (Harada et al., 2014). The time of feeding is another crucial factor to be considered in fed-batch fermentation. The suitable time to start the feeding is during substrate depletion or at the exponential phase where the growth of the cell starts to increase exponentially (Srivastava and Gupta, 2011). There is only one work reported from Qu et al. (2013) in tem of feeding strategy for improving the production of DHA in Schizochytrium sp. Three type substrate feeding strategies, including the intermittent feeding, constant speed feeding, and feed-back feeding, were studied experimentally. Fed-batch fermentation with optimized flow rate feeding which regulates the feed flowrate to enhance the process dynamically is still unexplored. Therefore, using this optimized strategy for the fed-batch fermentation process for the production of DHA should be studied more as it has the potential to increase the product yield.

However, high cost for optimization in the fermentation process is one of the issues that worrying in the research and development process. This is especially true because the chemical, material and machinery to conduct the fermentation process are costly due to the specificity (Wei Lan, 2015). This high cost is to ensure that the results obtained from the study is more accurate and increase the success of the experiment. A typical model based optimization approach, such as optimal control, in the fermentation process provides an alternative to find the optimal feed flowrate which helps reduce the research cost. Since the optimal control problem is solved numerically.

In fed batch process operations, the process variables undergo significant changes during the reaction (Seok, 2003). There are neither steady-state nor constant feed flowrate which the key variables can be regulated. Thus, the main target in fed batch operations is not to keep the system at some optimal constant feed flowrate, but rather to optimize trajectories that satisfy the objective function (Rohman et al. (2015, 2021). Optimal control approach which is able to optimize feed flowrate and times simultaneously, is used to allow for the computation despite the presence of constraints to ensure maximum DHA production is achieved.

In fact, contradictory objective functions have been found in this fed-batch fermentation process, i.e. maximum concentration and minimum process time which generates various combinations of optimal controls variables. The optimum results from the single-objective optimization problem cannot interpret the correlation between conflicting objective functions, and unable to provide a combination set of optimal trajectories. It is infeasible to determine a unique solution which is the optimal solution for all objectives simultaneously. Thus, it is suggested that application of a multi-objective optimal control (MOOC) approach for the improving optimal policy can offer a better way for predicting performance trade-offs emerging due to opposite actions of operating objectives for the fermentation process (Rohman and Aziz, 2020a). Notwithstanding this, the application of MOOC to the DHA production in fed-batch fermentation has been unexplored.

The multi-objective functions can also be recomposed as the unified objective optimization problem by using $\varepsilon-$constraint method. The practitioner (process engineer or analyst) selects a certain objective to be optimized, and the remaining objectives are converted as a constraint to be less than or equal to a pre-defined target value. The target values are being updated any time as a new single-objective optimization problem is solved (Rohman and Aziz, 2020b). On the other hand, the information of Pareto front can be generated in a single run optimization by using population-based non-linear programming methods. Among the alternatives, NSGA-II (Rohman and Aziz, 2020a) has shown to be very competitive. An algorithm's superior performance on a set of problems does not assure that it would perform similarly on a set of different problems. The comparative study on the performance of MOOC method is required. It provides a framework for researchers to come up with new strategy or modify the existing ones in order to achieve better results for certain case study.

In MOOC, finding the PF is not the only task – a good multi-objective algorithm should provide set of solutions that span the whole optimal PF as well as uniformly diverse in order to capture the configuration of optimal trade-off noticeably. Therefore, in order to determine the most effective MOOC method, the following criteria must be fulfilled: (i) Convergence: the most approximate Pareto solutions are imminent to the global Pareto optimal solutions; ii) Uniformity: the optimal solutions should be distributed evenly along the Pareto optimal frontier; (iii) Distribution: the set solutions should maintain diversity on the whole Pareto optimal frontier as much as possible. Performance matrices, such as hypervolume (HV), spacing (SP) and pure diversity (PD), can be used to assess those criteria (Rohman and Aziz, 2020b).

In this model based optimization (optimal control) technique, the construction of a mathematical model which can represent the fed-batch fermentation process is a must. However, it is difficult to develop such a model that corresponds to complete the DHA

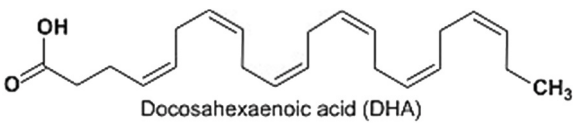

Fig. 1. Chemical structure of Docosahexanoic acid (Francotte, 2017).

fermentation process characteristic. The developed model should neither be too simple, which cannot represent the detailed behavior of the DHA fermentation, nor too accurate, which will provoke the complex computations. The fed batch process is a dynamic system which is presented as a set of ordinary differential equation (ODE) or differential algebraic equation (DAE). The optimal control technique is the most effective solution because it can deal with ordinary differential equations (ODE) and differential algebraic equations (DAE).

This paper's objective is carried out comparative study and to determine the most effective among two MOOC methods namely ε−constraint with HS, and NSGA-II to solve the MOOC problem in fed batch DHA fermentation process numerically. In the first part, the model of the DHA fed batch fermentation was developed and simulated in the MATLAB environment. The simulation results achieved were then compared with the actual data provided in the literature. Sensitivity analysis was also conducted in order to see the relation of various fermentation parameters to its performance.The next stage of the research is to determine the optimal control trajectories. The aim of this optimal control problem is to determine the optimal feed flowrate profiles to optimize the objective functions which are minimisation process time and maximization DHA concentration.

2. Mathematical model of fed-batch fermentation

2.1. Mass balance of fed-batch fermentation

Simulation of fermentation processes commonly presented as a plot of different state variables such as biomass, substrate and product against time (Bich, 1999). The fermentation process was profiled using differential equations describing the mass balance of the state variable. The diagram of fed-batch reactor is shown in Fig. 2.

The overall kinetic based on general mass balance can be described as in Equation (1) where V is the volume, y is the state variable, F_i is the inlet flow, y_i is the inlet concentration, F_{out} is the outlet flow, r_y is the reaction rate.

Change = Input – Output + Reaction

$$\frac{d(Vy)}{dt} = F_i y_i - F_{out} y + V\, r_y \tag{1}$$

Differentiation of the left-hand side of equation (1) gives equation (2) while the definition of the rate of volume change, dV/dt gives equation (3).

$$\frac{d(Vy)}{dt} = V\frac{dy}{dt} + y\frac{dV}{dt} \tag{2}$$

$$\frac{dV}{dt} = F_i - F_{out} \tag{3}$$

By inserting equation (2) and equation (3) in equation (1), it gives the general differential equation that can be used to represent the rate of change of the state variable against time in fed-batch fermentation process and also continuous fermentation process.

$$\frac{dy}{dt} = \frac{F}{V}(y_i - y) + r_y \tag{4}$$

The reaction rate term r_y replaced by equation (5) to represent the reaction constant and dilution rate, D was introduced to simplify the model.

$$r_y = q_y X \tag{5}$$

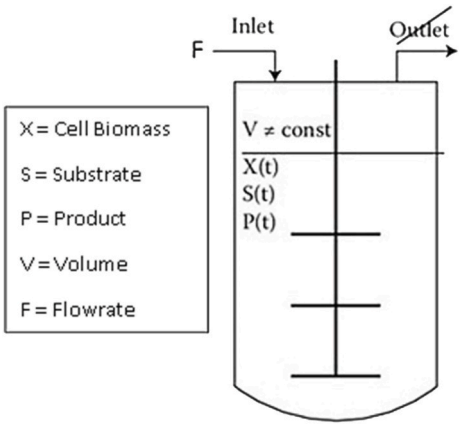

Fig. 2. The general mass balance component involves in fed-batch fermentation (Paulová et al., 2013).

$$D = \frac{F}{V} \tag{6}$$

q_y is the specific rate of reaction for state variable which includes u, the specific growth rate, q_s, substrate utilization rate and q_p, product formation rate. The differential equation for X, biomass, S, substrate and P, products were produced based on equation (4) and equation (5). In fed-batch fermentation, only substrate was added to the bioreactor, therefore input for biomass and product were ignored in the differential equation.

$$\frac{dX}{dt} = D(-X) + nX \tag{7}$$

$$\frac{dS}{dt} = D(S_i - S) - q_s \tag{8}$$

$$\frac{dP}{dt} = D(-P) + q_p X \tag{9}$$

$$\frac{dV}{dt} = F \tag{10}$$

To represent the model, specific rate of reaction n, q_s, q_p can be changed according to the kinetic parameter affecting the process. For the specific growth rate,u, Logistic equation was used to define the self-limiting growth of biological culture (Xu, 2019). *umax* represent maximum specific growth rate and X_m represent the maximum biomass concentration (Xu, 2019).

$$n = umaxX\left(1 - \left(\frac{X}{X_m}\right)\right) \tag{11}$$

For specific substrate utilization rate, q_s, kinetic parameter $y_{X/s}$, that represent yield of biomass on substrate and m, that represents the maintenance of the cell was inserted to show the substrate was utilized for the biomass growth and cell maintenance (Gahlawat and Srivastava, 2013).

$$q_s = \frac{1}{y_{x/s}}\, n + m \tag{12}$$

For specific product formation rates, Leudeking-Piret model is used. This model describes the formation of microbial products in function of cell growth rate and cell concentration (Niu et al., 2016). This model proposes two kinetic parameters which is α, product formation coefficient associated with cell growth rate and β, product formation coefficient associated with biomass concentration.

$$q_p = \alpha\, n + \beta \tag{13}$$

Kinetics in equations (11)–(13) were inserted into Equations (7)–(9) to derive the complete equation that will be used to represent the kinetic of the component in the fermentation process. Equation (17) was added to represent the change of volume over time in fed-batch fermentation kinetics.

$$\frac{dX}{dt} = D(-X) + \left[umaxX\left(1 - \frac{X}{X_m}\right)\right]X \tag{14}$$

$$\frac{dS}{dt} = D(S_i - S) - \left(\frac{1}{y_{x/s}}\, u + m\right) \tag{15}$$

$$\frac{dP}{dt} = D(-P) + (\alpha\, u + \beta)X \tag{16}$$

$$\frac{dV}{dt} = F \tag{17}$$

2.2. Model parameter estimation

To simulate the model, the value of each parameter needs to be determined. The parameter was estimated and adjusted to fit with the proposed model. The estimation of the kinetic parameters was performed by fitting the experimental data obtained from a study conducted by Qu et al. (2013) with the proposed model. The estimation was determined using non-linear regression analysis using *nlinfit* of MATLAB function.

2.3. Model validation and sensitivity analysis

Model validation was conducted towards the model to justify the accuracy of the data predicted from the proposed model with the experimental data obtained from a study conducted by Qu et al. (2013) through the fermentation process. Mean squared error (MSE)

analysis was done to assess the correlation between the predicted data obtained through the proposed model with the experimental data. The value of MSE was obtained by using Equation (18). The term n,$Yi$and $\hat{Y}i$ represents the number of the data point, the experimental data and predicted data.

$$MSE = \frac{1}{n}\sum_{i=1}^{n}(Yi - \hat{Y}i)^2 \tag{18}$$

R^2Besides that, R^2, the coefficient of determination was also calculated to validate the kinetic profile obtained through the model. R^2 was calculated by using Equation (19). The additional term in this equation include $\bar{y}_i$ which represent the mean value of Y.

$$R^2 = 1 - \frac{\sum (Yi - \hat{y}i)^2}{\sum (Yi - \bar{y}i)^2} \tag{19}$$

Afterward, sensitivity analysis was conducted by using one factor at a time method through validated model. One parameter was changed while other parameters remain constant to observe how significant the parameter change affect the cell growth, substrate utilization and product formation. The sensitivity of the parameter tested is 25% and 50% below and above the actual parameter value.

3. Multi-objective optimal control (MOOC) technique

3.1. The basic procedure of optimal control

The basic procedure of the optimal control approach is to transform the optimal control problem into NLP (Nonlinear Programming) by discretizing the control and/or the state variables. Then, the resulting finite-dimensional optimal control problem is solved by applying the NLP solver, i.e. enhanced scatter method to solve the optimal control problem directly. In this study, control vector parameterization (CVP) was applied where the control (feed flowrate) trajectory is discretized over a time interval, leaving the states (concentration) in the original form of ODE/DAE (ordinary/algebraic differential equation). The parameters which are used to discretize the control variable and the length of time subinterval are considered as the decision variables in optimal control problems. The objective functional evaluation is carried out by solving an initial value problem (IVP) of the original DAE system (Rohman et al., 2011, 2021)

Balsa-Canto et al. (2016) created the MATLAB code in AMIGO2 package for CVP algorithm, which was according to Vassiliadis et al.'s (1994) work. The standard procedure for the CVP method is represented as shown Fig. 3 (Rohman et al., 2011):

Problem.

$\underset{x,u(t),v(t)}{Min}\ \mu[d, U(t), V(t)]$ Objective function

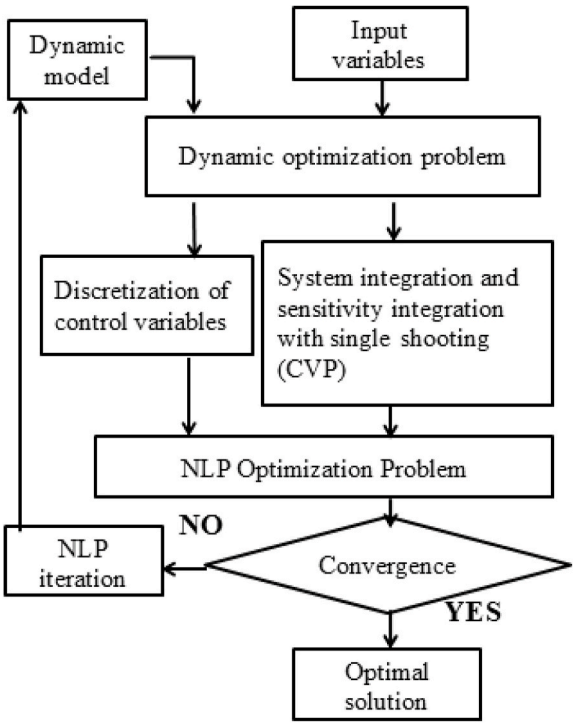

Fig. 3. Basic procedure of optimal control method: control vector parameterization.

$$\text{s.t. } g[d, U(t), V(t)] \leq 0 \quad \text{Inequality constraints}$$

$$c[d, U(t), V(t)] = 0 \quad \text{Equality constraints}$$

$$\frac{dZ}{dt} = F[x, U(t), V(t), t], t \in [0, 1] \quad \text{Process dynamic equation}$$

$$V(0) = V_0 \quad \text{Initial condition for states}$$

$$d^L \leq d \leq d^U \quad \text{Bounds for decision variables}$$

$$U^L \leq U \leq U^U \quad \text{Control profile bounds}$$

$$V^L \leq V(t) \leq V^U \quad \text{State profile bounds} \tag{20}$$

Step 1: Lagrange Interpolating Polynomial was employed to parametrize the control variables (CVs).

$$u_K(t) = \prod_{i=1}^{k} u_i \delta_i(t) \text{ where } \delta_i(t) = \prod_{1,i}^{K} \frac{(t - t_k)}{(t_i - t_k)}, u_K(t_i) = u_i, i = 1, \ldots, K \tag{21}$$

Step 2: The differential equation model was inserted the parameterized (CVs) from Step 1.

$$\frac{dV}{dt} = F(d, V(t), u_K(t), t) \quad with\ V(0) = V_0 \tag{22}$$

Step 3: Equation (10) represents the finite-dimensional optimization problem using the CVP method.

$$\underset{x,u(t),v(t)}{Min}\ \mu[d, U(t), V(t)]$$

$$\text{s.t. } g[d, U(t), V(t)] \leq 0$$

$$c[d, U(t), V(t)] = 0$$

$$\frac{dV}{dt} = F(d, V(t), u_K(t), t) \quad with\ V(0) = V_0$$

$$d^L \leq d \leq d^U$$

$$U^L \leq U \leq U^U$$

$$V^L \leq V(t) \leq V^U \tag{23}$$

Step 4: The starting conjecture for decision variables $\boldsymbol{d}$ and interval time t_i was replaced in the updated dynamic model, which was then addressed using an ODE solver (Runga-Kutta 4th order).

Step 5: The genetic algorithm (GA) or HS was used to execute the objective function and constraints in equation (23) that were assessed based on the values of $\boldsymbol{d}$ in step 4. Steps 4–5 should be repeated until convergence has been achieved.

3.2. Multi-objective optimization techniques

The optimum condition for MOOs is characterized as a set of solutions and a combination of optimal profiles defined as a non-dominated (ND) set or PF solutions. ND set is a certain set that is not dominated by any other solution that belongs to the solution set. The Pareto-optimal set which is the best option of the optimal solution for all objective functions is characterized by no improvement to a pre-defined objective without degenerating the solution of the second objective. The MOO techniques, which are able to provide the optimal PF and then being analyzed for application in the DHA fermentation process by practitioners, are described below (Sultana, 2016).

3.2.1. Multiple run approaches

In these approaches, the MOOC problem was solved at each iteration to yield non-dominated set. By sampling a set of discrete points and imposing non-dominated points obtained from multiple runs, the PF and the possible trade-off between objectives can be produced. The techniques considered was ε-constraint approach.

In the ε -constraint method, there was no accumulation in the single objective, instead the first objective was optimized while the second on was treated as constraint using threshold values ε. Therefore the problem:

$$\underset{x,u(t),z(t)}{Min}\ \mu_1[d, U(t), V(t)]$$

Subject to

$$\mu_2[d, U(t), V(t)] \leq \varepsilon$$

$$F[x, U(t), V(t), t] \in S \tag{24}$$

The optimal points on the Pareto-front were updated by progressively changing the ε for multiple runs (Maiti et al., 2011). For each optimizer run, nonlinear programming NLP solver was used for searching the optimal solution.

Two phase of NLP solvers which comprise of stochastic and deterministic based optimization was implemented as NLP solver. A population based method, such as Differential Evolution (DE) was applied as a stochastic-based NLP solver (Storn and Price, 1997). Meanwhile, the gradient based method, such as sequential quadratic programming (SQP), was used in terms of deterministic NLP solver. It should be noted that the deterministic (gradient based) is frequently multimodal and may converge to local optima, especially if they are started far away from the global solution, therefore, stochastic methods, i.e. DE, might be a good alternative to solve these difficulties as it has capability to escape from local solutions, locating the vicinity of the global optimum in reasonable computation times (Storn and Price, 1997). However, the stochastic method is usually generated refined solutions at a large computational cost. Since there is always a trade-off between convergence speed and robustness in both stochastic and deterministic methods, the HS is developed by adequately combining the key elements of a stochastic and a deterministic method, taking advantage of their complementary features (Rohman et al., 2016).

The HS is adopted from Banga et al. 's (2015) work and implemented in computer code by Balsa_Calder (2016), which divides into two successive phases. The near-global optimal solution was searched by DE solver in the first phase. The population searching step was switched to the second phase when a convergence criterion (SC1) based on the minimum searching step between each iteration occurred. Then, this solution is implemented as an initial point for the SQP solver in the final phase. As a convergence criterion (SC2) was fulfilled to reach an improved global optimal, the optimizer was stopped for searching iteration. The DE (SC1) and SQP (SC2) convergence criteria, which were specified as 0.02 and 10-6, are based on the empirical data for particular problem cases (Banga et al., 2015, Balsa_Calder, 2016). The basic flowchart of a hybrid strategy is shown in Fig. 4.

3.2.2. *Multi-objective genetic algorithms (MOGA)*

A MOGA manipulated a population of individuals to manage a procedure in which the population configurated the well-lined Pareto front in a single optimization run. Elitist Non-dominated Sorting GA or NSGA-II was one of widely used MOGA procedures which were developed by Deb et al. (2002). The flowchart of the NSGA-II is shown in Fig. 5. The NSGA-II implemented three features, i.e., elitist principle, explicit diversity preserving mechanism and non-dominated emphasizing. The individuals in a population were sorted and given ranks based on non-dominated criteria. The process selection was carried out by calculating the crowding distance which is the neighborhood cluster of a solution. Elitism was applied in the step that the ND individuals from the combination of parent and child population were propagated to the subsequent generation. The next step included off-springs generating from the selected population using crossover and mutation operators. Finally, the present off-springs and population were sorted dependent upon the non-domination and only the best individuals with the number of the population size (Hojjati et al., 2018).

3.3. *Problem optimal control formulation*

In this study, two different objective functions were considered: maximize DHA concentration, and minimize process time. The control (decision) variable was piece wise constant of feed flowrate. The X, biomass, S, substrate and P, products concentrations were

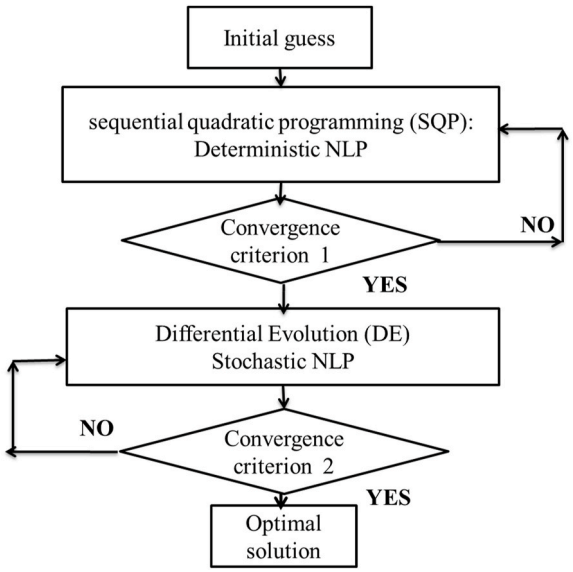

Fig. 4. Basic algorithm of the hybrid strategy.

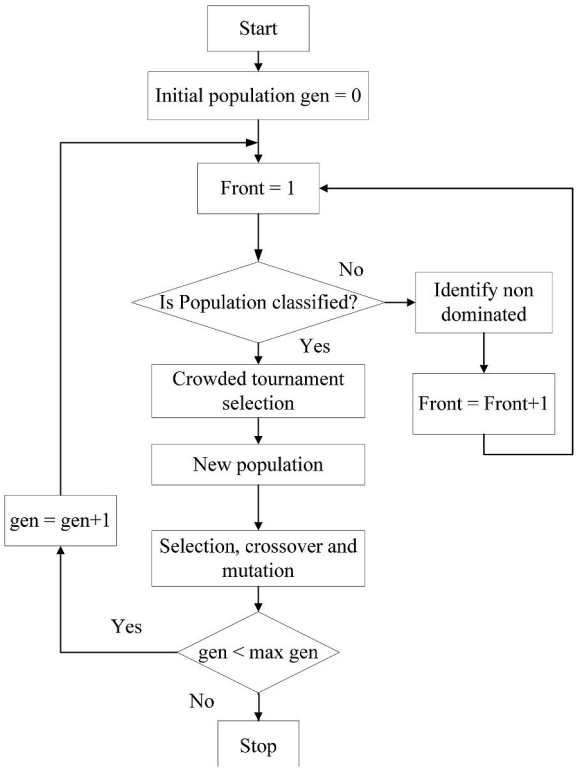

Fig. 5. The flowchart of NSGA-II algorithm (Hojjati et al., 2018) [25].

considered as states variables which were expressed as mass balance of selected operation mode. To maximize P, the max function is expressed as min -P. The upper and lower bounds implemented were the minimum and maximum capacity of the feed flowrate (0-6x 10^{-1} g/L.h). The control variable, time and time independent parameters are the components to be optimized.

MOOC Problem:

$$\underset{F}{\text{Min}} - \text{P}$$

$$\underset{F,\Delta t}{\text{Min}}\ t_f$$

Subject to: $M\dot{x}(t) = f(x(t), u(t), p, t)$(Equation (14)–(17))

$$0 \le F \le 6\text{x}10^{-1}\text{g/L.h}$$
$$0.5\ \text{h} \le \Delta t \le 10\ \text{h} \quad \text{(Lower and upper bounds)}$$

$$\text{V} \le 7\text{L} \quad \text{(Final inequality constraint)}$$

3.4. MOO performance metrics (quality indicators)

A statistical analysis on the ND points depicted from the PO solution was assessed the potency of the MOO techniques using performance metrics. Three quality indicators which was spacing (SP), hypervolume (HV) and pure diversity (PD) were considered to examine the performance metrics. The scatter of the ND points throughout the PF was accounted as SP. The HV metric is associated to the total of all the rectangular area shaped by any vector on the PF with reference to the objective space. PD was a performance metric to assess the diversity and uniformity of the PO. The description and mathematical fornulation of those metrics can be found in works of Zhang et al. (2017), Ibrahim, 2017 and Wang et al. (2017).

4. Results and discussion

The results comprehend model development and multi-objective optimal control of this fermentation reaction.

4.1. Model parameters estimation and simulation

Based on the mathematical model developed, the estimation of kinetic parameters was firstly performed by fitting the experimental data obtained from a study conducted by Qu et al. (2013) with the proposed model. The estimation was determined using non-linear regression analysis in the *nlinfit* of MATLAB function. The value of the kinetic parameters obtained from the estimation process is

shown in Table 1.

To simulate the mathematical model of fed-batch fermentation, the differential equations are solved by applying the 4th order Runge Kutta Method which is provided in the ode45 solver of MATLAB function. The state variable with an initial condition and the operating variable of the experiment used for the simulation process are summarized in Tables 2 and 3, respectively.

By inserting all the variables and parameters stated in Tables 1–3 to Equations (7)–(10), a complete set of the differential equation of the fed-batch system was obtained and solved simultaneously using ODE solver in POLYMATH software. Graph of predicted state variable concentration over time obtained from the simulation and the actual experimental data is shown in Fig. 6.

As can be seen in Fig. 6, the cell biomass and the DHA concentration increase until 60 h and become constant until 84 h. However, there is a slight decrease in the concentration of product and biomass at 24 h due to feeding of the substrate. For substrate utilization profile, the overall trend shows the substrate concentration decrease gradually until 60 h and then starts to increase until 84 h. Besides that, a slight increase in substrate concentration between 24 h and 36 h can be seen before it continues the decreasing pattern until 60 h.

In mathematical modelling, the model used is really important to represent and describe the process that happened in the reaction and provide good prediction towards the predicted data (Rivera et al., 2013). As for the fermentation process, the model used to determine the specific growth rate, β is very important as the specific growth rate will influence the substrate utilization and DHA formation. Different model used for α will describe different factors that will affect the specific growth rate such as the effect of substrate, temperature or pH towards the growth of the cell.

In this study, Logistic equation model is used to describe the specific growth rate. Logistic equation proposed that the growth of the cells are inhibited by the cell itself and independent towards the substrate (Muloiwa et al., 2020). Logistic model is one of the suitable models to predict the exponential growth phase kinetic (Sakthiselvan et al., 2020). Logistic equation shows a good fit based on the result obtained and can represent the experimental data. However, there is a slight difference of pattern between the common Logistic model trend which is sigmoid with the result obtained. A slight decrease in biomass concentration can be observed from the result after 24 h of fermentation. This is because the feeding that occurs at 24 h increases the initial culture volume which causes the concentration of biomass to be diluted slightly.

Next, Leudeking-Piret model was used to profile the DHA formation kinetic. Generally, the product formation was categorized into three different types which are growth-associated product, non-growth associated product and mixed growth-associated product (Sakthiselvan et al., 2020). In this study, DHA is the product of fermentation which can be categorized in mixed growth associated as DHA production is related to enhanced lipid and biomass accumulation (Zhang et al., 2018).

Therefore the terms β, growth-associated product formation coefficient and β, non-growth-associated product formation coefficient does not being neglected. From Table 1, the value of $Y_{X/s}$is 0.15 whereas the value of m is 0.001. The difference between these two values shows that the production of DHA in *Schizochytrium* sp. inclined towards the cell biomass growth more than towards non-growth metabolism. The low value of $Y_{p/s}$in the DHA production may be caused by the change of metabolism of the cell once the cell becomes senescence cell later in the fermentation process (Millner and Ekin, 2020). The change in metabolism may affect the lipid accumulation inside the *Schizochytrium* sp. cell. The DHA formation profile pattern follows the cell biomass growth but with lower concentration because DHA is a primary metabolite that is part of the cell itself.

For substrate utilization kinetics, two terms were included which is R^2, the yield constant of biomass over the substrate which represents the substrate utilization for biomass growth and R^2, maintenance coefficient which represents the substrate utilization for cell function other than the production of new biomass. This equation ignores the term F_i, the yield constant of product over substrate because DHA is a component of the biomass (Song et al., 2010). Generally, the substrate utilization profile is the opposite of the cell biomass growth profile. However, in the fed-batch, the concentration of substrate increases slightly in the middle of fermentation after a steady decrease because the substrate was fed and the rate of substrate utilization is lower than the rate of substrate added. When cell biomass enters the exponential phase, the substrate concentration decreases faster but then starts to increase after the cell enters the stationary phase. The increase of substrate is due to reduce substrate utilization by the cell as the cell started to be inhibited by the cell biomass itself as being proposed in the Logistic model.

4.2. Model validation

Based on the profiles of cell growth, substrate utilization and DHA production shown in Fig. 6, the proposed model can capture the reaction behavior with the $F_i$values of 0.9784, 0.9703 and 0.9666, respectively (see Table 4). Besides that, the MSE for the substrate utilization and DHA production with the model is quite low with values of 3.6924 and 0.5119 whereas for cell biomass growth is slightly high with value of 17.6791. The ≈ value approaching one with value of 0.9666 and above show that the predicted model has a

Table 1
Kinetic parameter value.

Kinetic Parameter	Symbol	Value	Unit
Maximum specific growth rate	*umax*	0.009	h^{-1}
Maximum biomass concentration	X_m	65	g/L
Yield constant (biomass/substrate)	$Y_{X/s}$	0.072	g/g
Maintenance coefficient	m	0.1	g/g.h
Growth-associated product formation coefficient	α	0.15	g/g
Non-growth-associated product formation coefficient	β	0.001	g/g.h

Table 2
State variable initial condition of the fed-batch *Schizochytrium* sp. fermentation process.

Variable	Symbol	Value	Unit
Initial cell biomass concentration	X(0)	4	g/L
Initial substrate concentration	S(0)	40	g/L
Initial product concentration	P(0)	0.05	g/L
Initial culture volume	V(0)	1	L

Table 3
Operating variable of the fed-batch *Schizochytrium* sp. fermentation process.

Parameter	Symbol	Value	Unit
Flow rate	F	0.1	g/L.h
Feed concentration	S_i	37	g/L

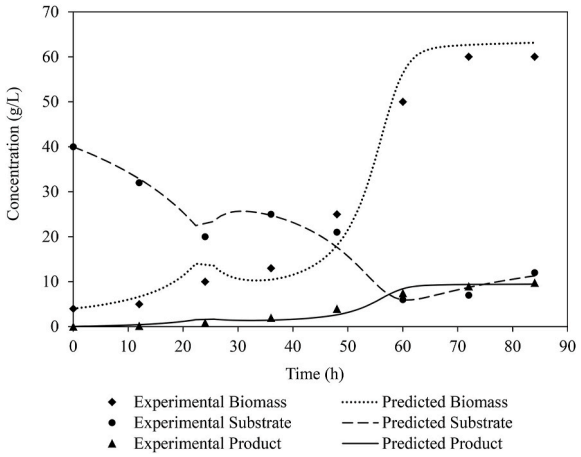

Fig. 6. Comparison between the profile of predicted state variable concentration over time and the actual experiment data.

Table 4
The value of mean squared error and coefficient of determination.

Kinetic profile	Coefficient of determination, R^2	Mean squared error, MSE
Cell biomass growth	0.9784	17.6791
Substrate utilization	0.9703	3.6924
Product formation	0.9666	0.5119

good fit with the actual experimental data for all three kinetic models. Besides that, the low value of MSE for substrate utilization and DHA formation which is lower than 5 shows that the error between the predicted data with the actual experimental data is low. However, the MSE for cell biomass kinetic profile is slightly high which suggests adjustment to the model can be done to improve the accuracy of the model.

4.3. Sensitivity analysis

The sensitivity analysis was done towards SP ≈ 0, the flow rate using one factor at a time method. This method only changes one parameter value at a time while other parameters were fixed using the same value as in Tables 1–3. Figs. 7–9 show the predicted profile of cell growth, substrate utilization and DHA formation throughout the fermentation process when the ≈ is changed by 25% and 50% above and below the actual value.

From Fig. 7, a low value of flowrate shows a faster increase in cell biomass and takes less time to reach maximum cell biomass concentration whereas a high flowrate takes more time to reach the maximum cell biomass concentration. This trend is caused by dilution which occurs as the feeding started at 24 h. As the flowrate increase, the dilution of the cell biomass also increases. Therefore, to reach the maximum cell growth faster, it is recommended to reduce the flow rate based on the proposed model.

Fig. 8 shows an almost similar pattern to Fig. 7 which is the lower the flow rate, the higher the DHA concentration in less time. The pattern of the DHA concentration is in Fig. 8 is also caused by the dilution. As the flowrate increase, the dilution towards the DHA concentration also increases as the total volume of fermentation increases. The slight difference of DHA formation profile with cell biomass growth profile can be seen that even after entering the stationary phase, the DHA concentration increase. During the stationary phase, the normal cell may become a senescent cell which is a condition where the cell has lost the ability to proliferate (Sasaki

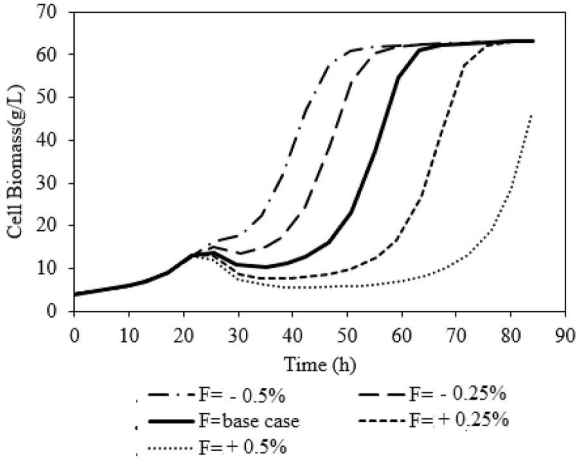

Fig. 7. Show the predicted cell growth profile at different flow rates.

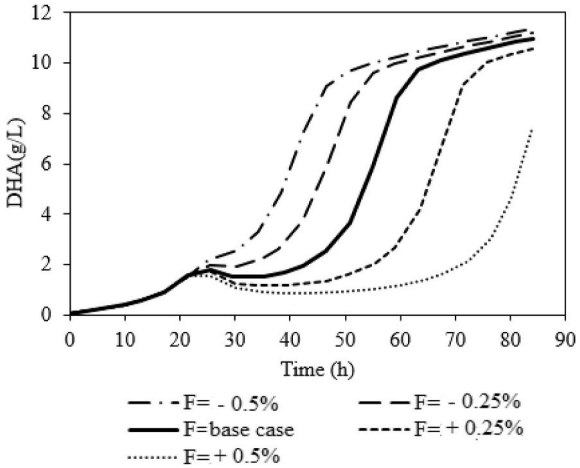

Fig. 8. Show the predicted DHA formation profile at different flow rate.

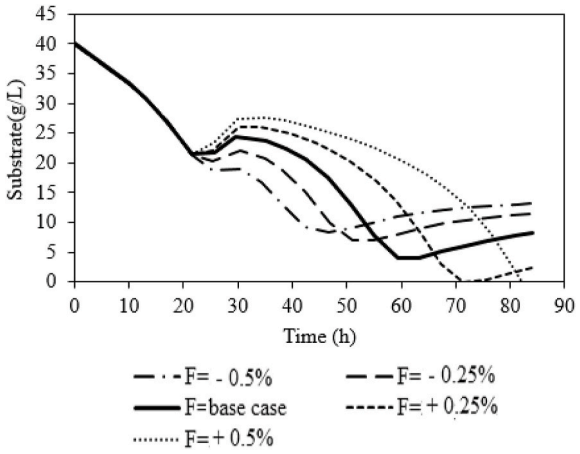

Fig. 9. Show the predicted substrate utilization profile at different flow rate.

and Nakanuma, 2013). The senescent cell still maintains metabolic activity and research shows that senescent cells display global alterations in lipid composition in the cell (Millner and Ekin Atilla-Gokcumen, 2020). DHA is a lipid and the increase of DHA at cell stationary cell growth phase may be caused by the metabolic activity that alters the lipid composition of the senescent cell.

Fig. 9 shows a few different patterns for the flow rate value. The substrate concentration decreases the same until 24h for each flow rate value inserted as the feed was not inserted yet. Then after 24 h, the substrate concentration increase slightly for the flow rate above – 0.25% whereas the substrate concentration temporarily becomes constant for −0.5%. After this phase, the pattern shows decreasing substrate concentration for all flow rate values before then increase again except for +0.5% which does not show an increase of substrate concentration even after 84 h. The increasing pattern shows that the substrate has been totally utilized by the cell while the feed is still inserted. For each flowrate, the substrate utilization rate is different. The lower the flow rate, the higher the substrate utilization. This can be seen in Fig. 9 where the lower flow rate has a faster increase in substrate concentration after 36 h.

In fed-batch fermentation, the kinetic of substrate utilization is heavily influenced by the feeding strategy. This is because generally during fed-batch fermentation, only substrate was fed during the fermentation process and no additional cell or product was inserted together. The constant flow rate feeding strategy provides a steady substrate supply to the cell biomass which caused an increase in the lag phase of the microbial cell (Elsayed et al., 2015). The constant flow rate feeding strategy also prevent the substrate from totally depleted which allow the cell biomass to get the carbon source continuously without waiting for any delay which can be observed in other feeding strategies.

4.4. Results of MOOC

The PF yielded from each MOO method was examined using performance metrics such as spacing SP, hypervolume HV, and pure diversity PD. Based on visual PF and performance metrics, effectual Pareto solutions with a decent condition of distribution, spread, and convergence to the optimal PF were assigned. Every optimal PF point was formed of a different feed flowrate profile. As a consequence, the points determined in the most effectual PF were also researched further.

4.4.1. Performance metrics analysis

Fig. 10 depicts the PF obtain by the NSGA-II and ε –constraint with HS techniques. For NSGA II, a population of 50 was used. In the meantime, the iteration count for weighted number and ε-constraint was also 50. Each iteration, with a different ε was carried out in accordance with the ε-constraint approach. As a result, the PFs resulted were composed of 50 distinct points. Table 5 summarises the performance metrics acquired from the three MOOC techniques, i.e. SP, HV and PD.

The PF obtained from the ε-constraint appears to be the most effectual preference ND points based on pictorial observation. Since the PO solutions were arrayed across the whole PF with more uniform arrangement and higher DHA concentration (11.45 g/L) at minimum time (72h).

The calculation of SP, HV, and PD of ND sets was performed in order to assess the effectiveness of PF in terms of distribution, convergence, and diversity. SP assessed the PF distribution indicator, which relates to the consecutive space between ND points. Table 5 shows that the ε constraint was the most equal distribution of PF related to the smallest value of SP. This is due to the fact that the SP metric sizes the standard deviation of disparities from the narrowest Euclidean space. When the ND points are in close proximity to one another, the respective space would be terse. As a matter of fact, all ND points of ε constraint are homogenous space apart as SP ≈ 0 (Zhang et al., 2017).

Besides that, the PD metric was employ to examine the multiplicity of un-reiterated solutions that are more disparity of ND points along the PF, inducing in a higher PD (Wang et al., 2017)[36]. ε constraint has the highest PD value, as shown in Table 5, indicating that the PF acquired was the most variant solution set.

The HV metric values in Table 5 account for both the PF's exactness and disparsity. This metric sums the volumes created by hypercubes assessed between a specified selected point W, i.e. the worst objective function values in objective space, and the particular

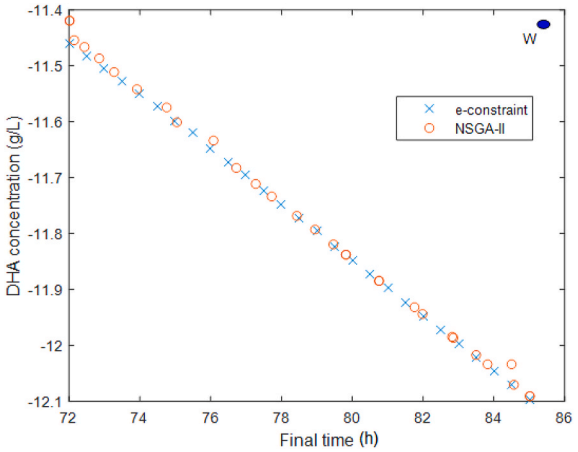

Fig. 10. PF of NSGA-II and ε constraint; W is point of worst objective functions.

Table 5
Results performance metrics of NSGA-II and epsilon ε constraint.

Metric	NSGA	e-constraint
PD	4.25 e3	5.20 e3
spacing	0.228	0.001
HV	4.320	4.436

ND point in PF. The HV indicator assesses an approximation's adjacency to the PF (Ibrahim, 2017). To put it another way, the nearer to reference point W, the nearer the solution gets to convergence, as shown in Fig. 10. As a consequence, the HV metric can acquire both the dispersed difference and the distance between the ND set and the ideal PF (convergence). Therefore, of the greatest HV attained, the ε constraint is the most precise and diversified solution set. This is due to the fact that the higher the HV, the better the approximation to the Pareto Optimal (PO) set (Ibrahim, 2017).

According to the results of the comparing study, the ε constraint was the most effectual MOO strategy. It is because the discovered solution set supplied the most exact, diversified, and appropriate in homogeneity allocation points along PF. Thereby, ε constraint was chosen to be incorporated for the following optimal trajectory study.

4.4.2. Optimal trajectories in PF analysis

Fig. 11 depicts the PF, i.e. ε-constraint, which is split into three zones. Lower *P* (DHA concentration) and shorter t_f were indicators of the lower end of the optimum PF (zone I). The upper end of the optimal PF (zone 3), on the other side, was denoted by a greater *P* and a longer t_f. The middling zone (zone 2), which was located between zones 1 and 2, was designated as moderate *P* and t_f. Fig. 11 depicts the ideal PF with varying flowrate track at each ND point. As shown in Fig. 12a-c, the ND points A, B, and C, which were located in zones 1, 2, and 3, respectively, exhibited variant tendency trajectories. Table .6 shows the outcomes of dynamic optimization for ND points A, B, and C, which are made up of two unique reactor performances such as *P* and t_f.

Table 6 presents that the t_f for respective ND points A, B, and C was 72h, 79h, and 83h. Since ND points A, B, and C, the respective *P* were11.45, 11.8, and 12.0. Feeding time and flowrate is a crucial factor that influences t_f and *S*, *P*. Because the reaction rates for the DHA and biomass elevate as flowrate climbed at a precise feeding time as substrate decrease significantly (Zhang et al., 2018, Millner and Ekin Atilla-Gokcumen, 2020). Feeding time of points A, B and C was 21h 24h and 26h, respectively. Thereby, the varying feeding tracks result in a change in the amount of t_f and *S, P*, as indicated in Fig. 12a, b, and 12c. As the feed flowrate in point C is quite low, the dilution towards the P concentration decreases. Then, the higher final P concentration is obtained. It is also denoted from Fig. 12 that the longer t_f depletes the unreacted S, which in sequence generates the larger P. This is because the cell requires a longer time to reach the exponential phase and fully utilize the substrate to proliferate. The ability of practitioners to propose preference is strongly linked to the implementation of PF analysis. Because ND points have a disparate optimum feed flowrate tracks, practitioners can use the PF to decide which amount of P and tf can be traded off to get the most suitable operating conditions for the fed-batch fermentation. The derived PF of ε-constraint obviously presents several possibilities to the decision maker in order to apply the optimum trajectories related to practical and decent considerations.

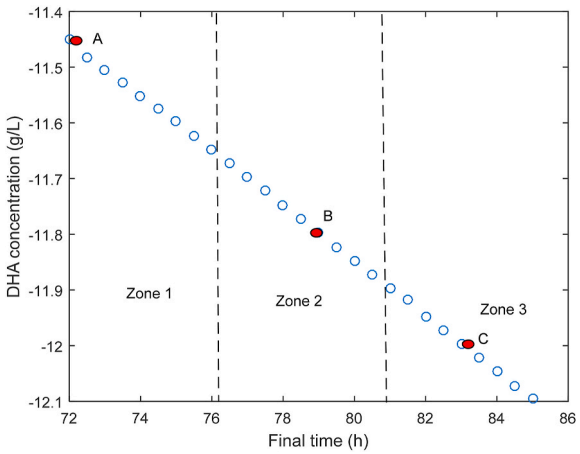

Fig. 11. PF obtained by ε-constraint with the zones and selected non-dominated points.

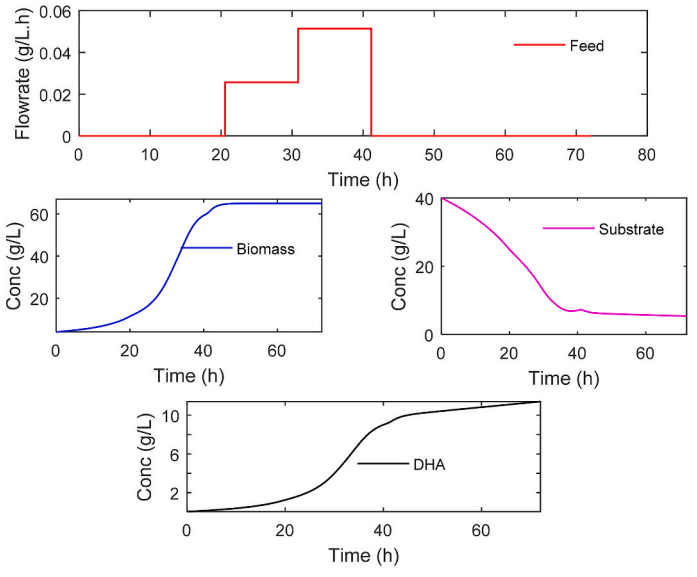

(a) Point A

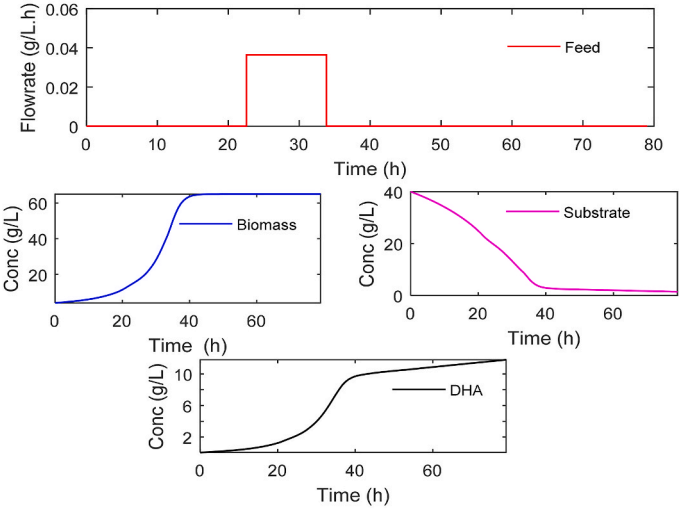

(b) Point B

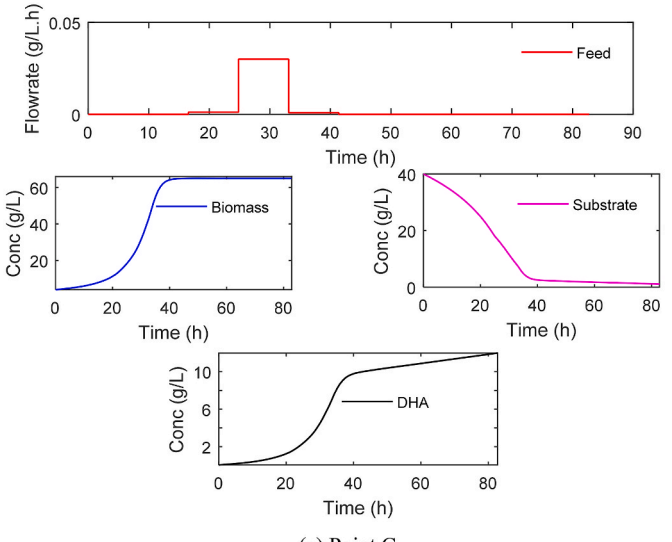

(c) Point C

(caption on next page)

Fig. 12. Optimal feed flowrate and concentrations in point A, B and C.

Table 6
t_f and DHA, substrate concentrations in point A, B and C.

	Point A	Point B	Point C
Final time (h)	72	79	83
P, DHA concentration (g/L)	11.45	11.80	12.0
S, Concentration of unreacted substrate (g/L)	5.36	1.44	1.09

5. Conclusion

The kinetic model of cell biomass growth, substrate utilization and DHA formation proposed in the study fit decently with the experimental data of constant flow rate feeding mode in fed-batch fermentation of Schizochytrium sp when using the estimated kinetic parameter with the R^2 value of 0.9784, 0.9703 and 0.9666 and MSE value of 17.6791, 3.6924, 0.5119. The model proposed can be used to solve optimal control problem. Besides that, the sensitivity analysis shows the model could predict the profile of all three state variables using different flowrate.

DHA production in a fed-batch process is distinguished by the occurrence of conflicting performance targets. As a result, fed batch optimal control issues must simultaneously address maximization DHA production and minimisation final time for the optimal trade-off solutions. This work provides insight into the possibility of using multi-objective optimal control in a fed-batch fermentation. The e-constraint with hybrid strategy, and elitist non-dominated sorting genetic algorithm or NSGA-II techniques have been reviewed and contrasted in order to find the best PF for MOOC involving P and t_f. The numerical results, when compared to all data obtained with various performance indicators, such as SP, PD, and HV, show that the ε-constraint approach is better to the NSGA-II in terms of the final PF's convergence (HV) and diversity.

Each ND point has a variant optimal feeding time and feed flowrate track, resulting in a varied quantity of P and t_f. The practitioners can use the information from each optimal point along the PF to make trade-offs between competing objectives and pick a suitable operating tracks for the process.

Declaration of competing interest

The authors declare that they have no known competing financial interests or personal relationships that could have appeared to influence the work reported in this paper.

Data availability

The authors are unable or have chosen not to specify which data has been used.

References

Balsa-Canto, E., Henriques, D., Gábor, A., Banga, J.R., 2016. AMIGO2, a toolbox for dynamic modeling, optimization and control in systems biology. Bioinformatics 32, 3357–3359.
Banga, J.R., Balsa-Canto, E., Moles, G., Alonso, A.A., 2015. Dynamic optimization of bioprocesses: efficient and robust numerical strategies. J. Biotechnol. 117, 407–419.
Bich, P.T., 1999. Modelling and Control of Microbii Fed-Batch and pH-Auxcxstat Processes.
Calder, P.C., 2016. Docosahexaenoic acid. Ann. Nutr. Metabol. 69 (1), 8–21.
Deb, K., Pratap, A., Agarwal, S., Meyarivan, T., 2002. A fast and elitist multi-objective genetic algorithm: NSGA-II,Evolutionary Computation. IEEE Transac. 6, 182–197.
Dominguez, L.J., Barbagallo, M., 2018. Not all fats are unhealthy. In: The Prevention of Cardiovascular Disease through the Mediterranean Diet. Elsevier, pp. 35–58.
Elsayed, E.A., Omar, H.G., El-Enshasy, H.A., 2015. Development of fed-batch cultivation strategy for efficient oxytetracycline production by Streptomyces rimosus at semi-industrial scale. Braz. Arch. Biol. Technol. 58 (5), 676–685.
Francotte, E.R., 2017. Practical aspects and applications of preparative supercritical fluid chromatography. In: Supercritical Fluid Chromatography: Handbooks in Separation Science. Elsevier Inc, pp. 275–315.
Gahlawat, G., Srivastava, A.K., 2013. Development of a mathematical model for the growth associated Polyhydroxybutyrate fermentation by Azohydromonas australica and its use for the design of fed-batch cultivation strategies. Bioresour. Technol. 137, 98–105.
Harada, Y., Sakata, K., Sato, S., Takayama, S., 2014. Fermentation pilot plant. In: Fermentation and Biochemical Engineering Handbook: Principles, Process Design, and Equipment, third ed. Elsevier Inc, pp. 3–15.
Hishikawa, D., Valentine, W.J., Iizuka-Hishikawa, Y., Shindou, H., Shimizu, T., 2017. Metabolism and functions of docosahexaenoic acid-containing membrane glycerophospholipids. FEBS (Fed. Eur. Biochem. Soc.) Lett. 591, 2730–2744.
Hojjati, A., Monadi, M., Faridhosseini, A., Mohammadi, M., 2018. Application and comparison of NSGA-II and MOPSO in multi-objective optimization of water resources systems. J. Hydrol. Hydromechanics 66, 323–329.
Ibrahim, A., 2017. Toward Enhancement of Evolutionary Multi- and Many-objective Optimization: Algorithms, Performance Metrics, and Visualization Techniques. Thesis, University of Ontario Institute of Technology.
Maiti, S.K., Lantz, A.E., Bhushan, M.B., Wangikar, P.P., 2011. Multi-objective optimization of glycopeptide antibiotic production in batch and fed batch processes. Bioresour. Technol. 102, 6951–6958.
Millner, A., Ekin Atilla-Gokcumen, G., 2020. Lipid players of cellular senescence. Metabolites 10 (9), 1–17.
Muloiwa, M., Nyende-Byakika, S., Dinka, M., 2020. Comparison of unstructured kinetic bacterial growth models. S. Afr. J. Chem. Eng. 33 (May 2019), 141–150.
Niu, D., Zhang, L., Wang, F., 2016. Modeling and parameter updating for nosiheptide fed-batch fermentation process. Ind. Eng. Chem. Res. 55 (30), 8395–8402.
Paulová, L., Patáková, P., Brányik, T., 2013. Advanced Fermentation Processes, pp. 89–110. May 2014.

Qu, L., Ren, L.J., Sun, G.N., Ji, X.J., Nie, Z.K., Huang, H., 2013. Batch, fed-batch and repeated fed-batch fermentation processes of the marine thraustochytrid schizochytrium sp. for producing docosahexaenoic acid. Bioproc. Biosyst. Eng. 36 (12), 1905–1912.
Rivera, E.C., Yamakawa, C.K., Garcia, M.H., Geraldo, V.C., Rossell, C.E.V., Filho, R.M., Bonomi, A., 2013. A procedure for estimation of fermentation kinetic parameters in fed-batch bioethanol production process with cell recycle. Chem. Eng. Transac. 32, 1369–1374.
Rohman, F.S., Sata, S.A., Othman, M.R., Aziz, N., 2021. Dynamic optimization of autocatalytic esterification in semi-batch reactor. Chem. Eng. Technol. 44, 648–660.
Rohman, F.S., Aziz, N., 2020a. Multi-objective optimization of batch electrodialysis for minimizing energy consumption by using non-dominated sorting genetic algorithm (NSGA-II). IOP Conf. Ser. Mater. Sci. Eng. 736, 032005.
Rohman, F.S., Aziz, N., 2020b. Performance metrics analysis of dynamic multi-objective optimization for energy consumption and productivity improvement in batch electrodialysis. Chem. Eng. Commun. 208, 517–529.
Rohman, F.S., Sata, S.A., Aziz, N., 2016. Online dynamic optimization strategy for handling disturbance in semi batch Autocatalytic esterification process: application of hybrid optimizer and simple Re-optimization activator. Adv. Sci. Lett. 22, 2729–2733.
Rohman, F.S., Abdul Sata, S., Aziz, N., 2015. Maximizing profit of semi batch Autocatalytic esterification process in the presence of disturbance: application of cascaded-conditional based online dynamic optimization. Comput. Aid. Chem. Eng. 37, 1625–1630.
Rohman, F.S., Sata, S.A., Aziz, N., 2011. Dynamic Optimization of Autocatalytic Esterification in Semi Batch Reactor Using Orthogonal Collocation and Control Vector Parameterization Method. World Congress on Engineering and Technology, pp. 1–4. CET2011.
Sakthiselvan, P., Sudharsan Meenambiga, S., Madhumathi, R., 2020. Kinetic studies on cell growth. In: Cell Growth. IntechOpen.
Sasaki, M., Nakanuma, Y., 2013. Pathogenesis of bile duct lesions in primary biliary cirrhosis: role of autophagy followed by cellular senescence. In: Autophagy: Cancer, Other Pathologies, Inflammation, Immunity, Infection, and Aging. Elsevier Inc, pp. 293–303.
Seok, J., 2003. Hybrid adaptive optimal control of anaerobic fluidized bed bioreactor for the de-icing waste treatment. J. Biotechnol. 102, 165–175.
Song, X., Zhang, X., Kuang, C., Zhu, L., Zhao, X., 2010. Batch kinetics and modeling of DHA production by S. limacinum OUC88. Food Bioprod. Process. 88 (1), 26–30.
Srivastava, A.K., Gupta, S., 2011. Fed-batch fermentation - design strategies. In: Comprehensive Biotechnology, , second ed.vol. 2. Elsevier Inc, pp. 515–526.
Storn, R., Price, K., 1997. Differential evolution - a simple and efficient heuristic for global optimization over continuous spaces. J. Global Optim. 11 (4), 341–359.
Sultana, R., 2016. Application of Genetic Algorithm in Multi-Objective Optimization of an Indeterminate Structure with Discontinuous Space for Support Locations. Grand Valley University.
Vassiliadis, V.S., Sargent, R.W.H., Pantelides, C.C., 1994. Solution of a class of multistage dynamic optimization problems. 1. problems without path constraints, 2. problems with path constraints. Ind. Eng. Chem. Res. 33 2111 (2122), 2123–2133.
Wang, H., Jin, Y., Yao, X., 2017. Diversity assessment in many-objective optimization. IEEE Trans. Cybern. 47, 323–329.
Wei Lan, J.C., 2015. The optimization of docosahexaenoic acid production from waste by Schizochytrium limacinum SR21. J. Biotechnol. 208, S33.
Xu, P., 2019. Analytical Solution for a Hybrid Logistic-Monod Cell Growth Model in Batch and CSTR Culture. BioRxiv.
Zhang, S., Li, S., Harley, R.G., Habetler, T.G., 2017. Performance evaluation and comparison of multi-objective optimization algorithms for the analytical design of switched reluctance machines. CES Transac. Electr. Mach. Syst. 1, 58–65.
Zhang, M., Wu, W., Guo, X., Weichen, Y., Qi, F., Jiang, X., Huang, J., 2018. Mathematical modeling of fed-batch fermentation of Schizochytrium sp. FJU-512 growth and DHA production using a shift control strategy. 3 Biotech 8 (3), 162.